

# Electronic properties of $\text{AlVO}_4$ for gas sensor applications

Salvador Antonio Palomares-Sánchez ·  
Yuri M. Chumakov · Selina Ponce-Castañeda ·  
Bernard E. Watts · Fabrizio Leccabue · Gabrielle Bocelli

Received: 8 February 2007 / Accepted: 23 April 2007 / Published online: 19 July 2007  
© Springer Science+Business Media, LLC 2007

**Abstract** The binary oxide  $\text{AlVO}_4$  is being proposed as a new gas sensor material. An X-ray investigation, IR spectrum analysis, resistivity and a calculation of the electronic structure of this compound have been carried out in order to determine its structural, absorptive and sensor properties. The fragment  $[\text{Al}_3\text{V}_3\text{O}_{23}]^{18-}$  is the chain chosen to study the electronic properties of  $\text{AlVO}_4$  in the framework of the frontier orbital theory and the interaction between molecules has been described by the Molecular Electrostatic Potential (MEP). The vibration analysis and the simulated infrared spectrum (IR) were calculated for the unit  $[\text{Al}_3\text{V}_3\text{O}_{23}]^{18-}$  and a comparative analysis with the experimental spectrum of  $\text{AlVO}_4$  is also presented.

## Introduction

Metal orthovanadates find wide technological application as catalysts, laser hosts, masers, and phosphors. Oxides such

as  $\text{TiO}_2$  and  $\text{SnO}_2$  are used as the active semiconductor in gas sensors since they have advantages such as stability and low cost, however, they are unselective to different gases. Thus, the orthovanadate  $\text{AlVO}_4$  (I) has captured some attention for its selective detection of NO and  $\text{NO}_2$ . The sensitivities,  $\sigma/\sigma_{\text{air}}$ , reported of the mixture for NO and  $\text{NO}_2$  at 400 °C are 2.54 and 2.71, respectively [1, 2]. Mixtures of  $\text{AlVO}_4$ -ZnO- $\text{V}_2\text{O}_5$  have also been studied in order to establish their sensor properties to detect  $\text{NO}_x$  gases [2]. Also density functional calculations on structure and vibrational properties of bulk  $\text{AlVO}_4$  have been carried out [3].

Preparation methods, notably sol-gel, RF sputtering and pulsed laser ablation deposition are used to prepare Al-V-based oxide semiconductors, both in powder and thin film forms, have been reported; some experimental studies have been also carried out in order to determine its structural, absorptive and sensor properties [4–9]. It is not clear whether pure  $\text{AlVO}_4$  is the responsible for the sensor properties or a mixture of  $\text{AlVO}_4$ ,  $\alpha$ - $\text{Al}_2\text{O}_3$  and Al-V-O spinel phase [4].

In this work single phase  $\text{AlVO}_4$  has been prepared in powder and in thin film forms, by sol gel processing X-ray diffractometry, infrared spectroscopy, and resistivity measurements have been carried out to determine the structural, absorptive and potential sensor activity. A calculation of the electronic structure of  $\text{AlVO}_4$ , has also been made to gain a better understanding of its possible catalytic properties.

The vibrational analysis and simulated infrared spectrum (IR) were calculated for the unit  $[\text{Al}_3\text{V}_3\text{O}_{23}]^{18-}$  and compared with the experimentally determined infrared spectrum. The electrical characterization in air of the  $\text{AlVO}_4$  films deposited by sol gel route on alumina substrate is also presented.

---

S. A. Palomares-Sánchez (✉)  
Facultad de Ciencias, UASLP, Alvaro Obregón 64,  
78000 San Luis Potosi, SLP, Mexico  
e-mail: sapasa04@fciencias.uaslp.mx

Y. M. Chumakov  
Institute of the Applied Physics, Academy of Sciences of  
Moldova, Academy Str. 5, 2028 Kishinev, Moldova

S. Ponce-Castañeda  
Universidad Politécnica de San Luis Potosí, Iturbide 140,  
78000 San Luis Potosi, SLP, Mexico

B. E. Watts · F. Leccabue · G. Bocelli  
IMEM/CNR, Area delle Scienze 37/a, 43010  
Loc. Fontanini (Parma), Italy

## Experimental

### Preparation of $\text{AlVO}_4$ powders

The sol gel method was used to prepare both powders and thin films. 5.1 g of  $\text{Al}(\text{O}^i\text{Pr})_3$  was dissolved in 20 mL of toluene, at room temperature; 5 mL of toluene was added to 6.1 g of  $\text{VO}(\text{O}^i\text{Pr})_3$  in a second beaker. The two solutions were mixed and stirred in a dry air glove-box. The solution was transferred to a three necked round bottom flask and refluxed for 6 h under flowing nitrogen. The initial yellow solution became dark green at the end of the refluxing and, finally, diluted to a volume of 50 mL with toluene in a glove box. An aliquot of the Al–V–O–toluene solution and isopropyl alcohol in a volume ratio 1:5 was heated up to 350 °C on a hot plate for 10 min. The powders were calcinated in a furnace at 650 °C for 120 min.

### Thin film deposition

A spin-on technique was used to deposit thin films onto polycrystalline alumina substrates. The solution of  $\text{Al}^{3+}$  and  $\text{V}^{5+}$  in toluene was diluted with isopropyl alcohol, in ratios of 1:1, 1:3 and 1:5. The three solutions were syringed through a 0.2  $\mu\text{m}$  Teflon filter and dropped onto polycrystalline alumina. Spin coating was performed at 3,000 rpm for 1 min. The gelled films were left to dry for 48 h and then annealed at 600 °C for 20 min. Three different thin films (ALVO9, ALVO10 and ALVO11) have been obtained from these dilute solutions.

X-ray powder diffraction data were collected, using a Philips PW 1050/25 modified diffractometer with  $\text{CuK}_\alpha$  radiation, for values of  $2\theta$  from 3 to 90°, with a step width of 0.05° and a count time of 2.0 s/step, for each specimen. The X-ray diffraction spectrum of the ALVO9 film is shown in Fig. 1 together with the spectrum of pure  $\text{AlVO}_4$  powder (lower graph). It is possible to associate the peaks of the spectrum of the film to the main peaks of the  $\text{AlVO}_4$ .

### X-ray analysis and IR spectrum

Figure 2 shows the X-ray spectrum of the powder, indicating that  $\text{AlVO}_4$  is the only phase present. A Rietveld refinement was used to find the structural parameters of this compound. Although the actual structure of  $\text{AlVO}_4$  has not been determined, the use of the structural parameters of the  $\text{FeVO}_4$ , using a MAUD program [10], produced a very good fit between the experimental and simulated spectrum. The triclinic space group P-1 and the atomic positions reported in Ref. [11] were assumed for the initial structural model. Table 1 shows the refined structural parameters compared with the corresponding data reported in the literature. Table 2 reports the refined atomic positions

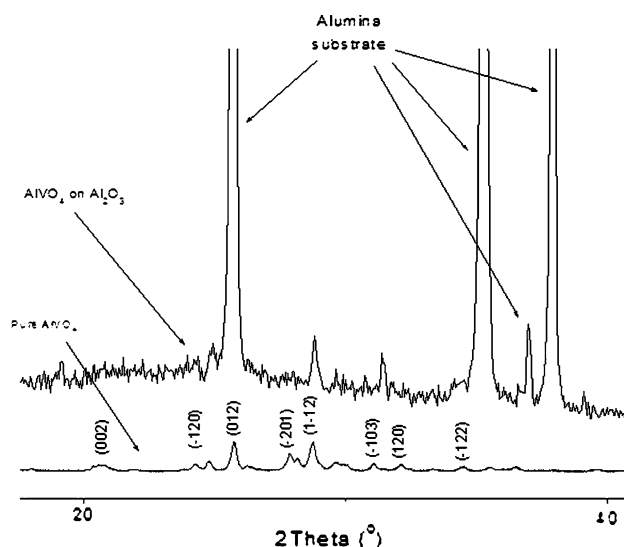


**Fig. 1** X-ray spectrum of  $\text{AlVO}_4$  thin film (ALVO9) compared with the corresponding one of  $\text{AlVO}_4$  powders

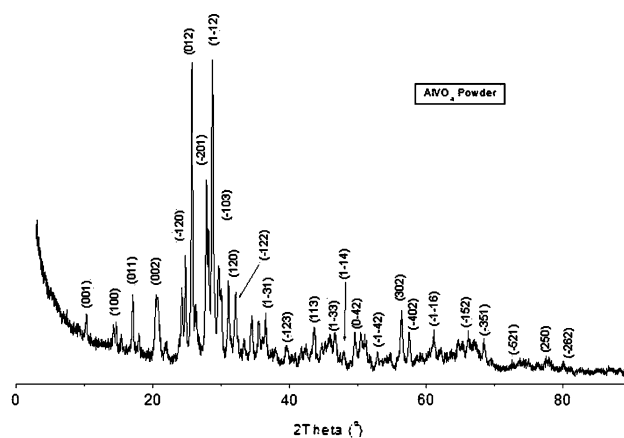


**Fig. 2** X-ray diffraction spectrum of  $\text{AlVO}_4$  powders

obtained, which were used as the coordinates of the atomic positions of the chain to examine the electronic properties of  $\text{AlVO}_4$ .

Figure 3 reports the experimental IR spectrum obtained using a Nicolet Avatar 360 FT-IR spectrometer by applying the KBr disc technique.

### Electrical characterization

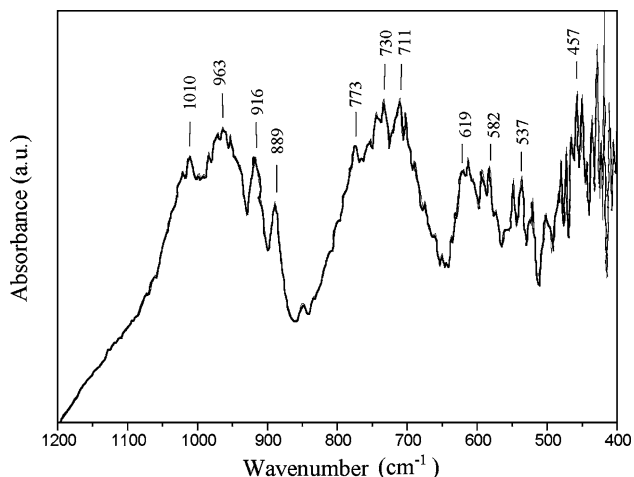
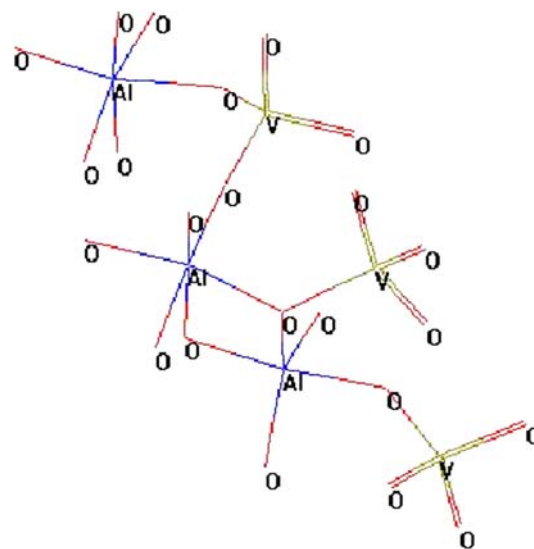
Gold electrodes were evaporated on the surface of the films in order to perform the electrical characterization by the Van der Pauw method. The samples were attached to a heater block collocated in a vacuum chamber and then the resistivity was measured as a function of temperature, between 290 and 402 K. The resistivity of  $\text{AlVO}_4$  at room temperature was found to be  $1.04 \times 10^4 \Omega \text{ cm}$ . The temperature coefficient of resistivity is  $\alpha = -2.9099 \times 10^{-3} \text{ }^\circ\text{C}^{-1}$  and the activation energy is  $E_a = 0.11 \text{ eV}$  [11].

**Table 1** Refined cell parameters of  $\text{AlVO}_4$  (space group P-1)

|                       | Ref. [11] | Ref. [9] | Ref. [8] | This work |
|-----------------------|-----------|----------|----------|-----------|
| $a$ (nm)              | 0.6538    | 0.6471   | 0.6480   | 0.6544    |
| $b$ (nm)              | 0.7756    | 0.7742   | 0.7750   | 0.7760    |
| $c$ (nm)              | 0.9131    | 0.9084   | 0.9084   | 0.9142    |
| $\alpha$ ( $^\circ$ ) | 96.170    | 96.848   | 96.848   | 96.26     |
| $\beta$ ( $^\circ$ )  | 107.230   | 105.825  | 105.825  | 107.22    |
| $\gamma$ ( $^\circ$ ) | 101.400   | 101.399  | 101.399  | 101.43    |

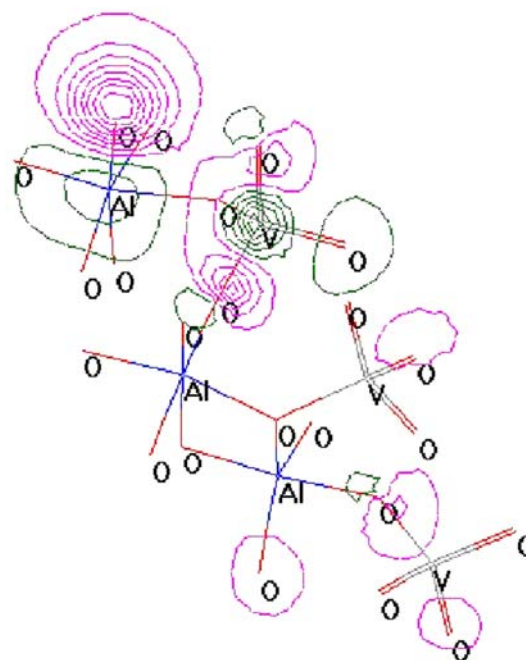
**Table 2** Atomic positions of Al, V and O in  $\text{AlVO}_4$ 

| Atom | $x/a$   | $y/b$    | $z/c$   | $U_{\text{iso}}$ |
|------|---------|----------|---------|------------------|
| Al1  | 0.78441 | 0.70756  | 0.38718 | 2.74363          |
| Al2  | 0.44425 | 0.894780 | 0.20253 | 4.62962          |
| Al3  | 0.96501 | 0.29202  | 0.00458 | 0.26217          |
| V1   | 0.00872 | 0.99386  | 0.25180 | 4.77324          |
| V2   | 0.21273 | 0.60352  | 0.34498 | 3.18048          |
| V3   | 0.52802 | 0.29755  | 0.11548 | 2.28797          |
| O1   | 0.62519 | 0.48470  | 0.28008 | 0.82893          |
| O2   | 0.25638 | 0.40600  | 0.41489 | 6.80894          |
| O3   | 0.08995 | 0.70437  | 0.43782 | 1.74601          |
| O4   | 0.13070 | 0.06776  | 0.42920 | 10.77737         |
| O5   | 0.51943 | 0.79088  | 0.36824 | 4.34504          |
| O6   | 0.75842 | 0.88696  | 0.27149 | 0.05620          |
| O7   | 0.52346 | 0.13606  | 0.23540 | 4.54421          |
| O8   | 0.18672 | 0.88366  | 0.19103 | 13.44315         |
| O9   | 0.37393 | 0.72839  | 0.04575 | 1.07764          |
| O10  | 0.27008 | 0.29892  | 0.05925 | 1.24308          |
| O11  | 0.93115 | 0.11064  | 0.13167 | 12.19090         |
| O12  | 0.04922 | 0.49520  | 0.14970 | 3.69444          |

**Fig. 3** Infrared spectrum of  $\text{AlVO}_4$  powders between 1,200 and 400  $\text{cm}^{-1}$ **Fig. 4**  $[\text{Al}_3\text{V}_3\text{O}_{23}]^{18-}$  chain used to study the electronic properties of  $\text{AlVO}_4$ 

### Theoretical analysis

A quantum-chemical study of the electronic structure of  $\text{AlVO}_4$  and the simulation of the IR spectrum were performed in order to investigate the sensor properties. The  $[\text{Al}_3\text{V}_3\text{O}_{23}]^{18-}$  chain, chosen to study the electronic properties of  $\text{AlVO}_4$  is illustrated in Fig. 4. The atomic coordinates were taken after the Rietveld refinement of the experimental spectrum of  $\text{AlVO}_4$ . The  $[\text{Al}_3\text{V}_3\text{O}_{23}]^{18-}$

**Fig. 5** HOMO for  $[\text{Al}_3\text{V}_3\text{O}_{23}]^{18-}$

consists of two different pentagonal ( $\text{AlO}^{5-}$ ) and one hexagonal ( $\text{AlO}^{6-}$ ) polyhedra and three different tetragonal ( $\text{VO}^{4-}$ ) polyhedra. This study was performed in the framework of the frontier orbital theory that considers the interaction between Highest Occupied Molecular Orbital (HOMO) and Lowest Unoccupied Molecular Orbital (LUMO) [12]; for reagents, these orbitals have the smallest energy separation and they can overlap most. The electronic structure of  $\text{AlVO}_4$  has been explored by the ZNDO/1 method [13] using the HyperChem 7.0 program and, then, the vibration analysis was performed.

The contour maps of the HOMO and LUMO for  $[\text{Al}_3\text{V}_3\text{O}_{23}]^{18-}$  are represented in Figs. 5, 6, respectively. The region of the highest density (regardless of sign) is generally the site of electrophilic attack; the oxygen atoms, which are connected to six-coordinated atoms of Al and one of the V atoms, are in such sites. The interaction between molecules was conveniently characterized using the Molecular Electrostatic Potential (MEP). The results of the electrostatic potential calculations can be used to predict initial attack positions of protons or other ions. The MEP distribution analysis of  $[\text{Al}_3\text{V}_3\text{O}_{23}]^{18-}$  shown in the Fig. 7 shows that the reaction sites are located mainly in the regions of the ( $\text{AlO}^{6-}$ ) polyhedra. Thus, considering the contour maps of the HOMO and distribution of the MEP, the interaction between  $[\text{Al}_3\text{V}_3\text{O}_{23}]^{18-}$  and  $\text{NO}_2$  groups could occur according to the scheme represented in Fig. 8.

The vibrational frequencies of the simulated infrared spectrum for  $[\text{Al}_3\text{V}_3\text{O}_{23}]^{18-}$  are derived from the harmonic approximation, which assumes that the potential surface has a quadratic form. Table 3 shows the main atomic groups (Al–O and V–O bonds) that contribute to the

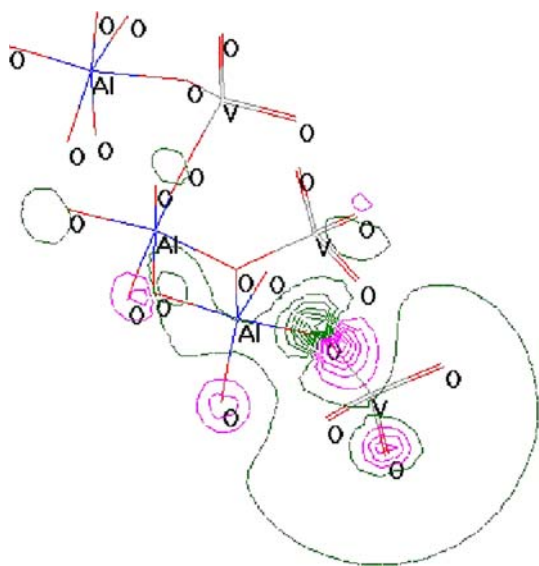


**Fig. 6** LUMO for  $[\text{Al}_3\text{V}_3\text{O}_{23}]^{18-}$

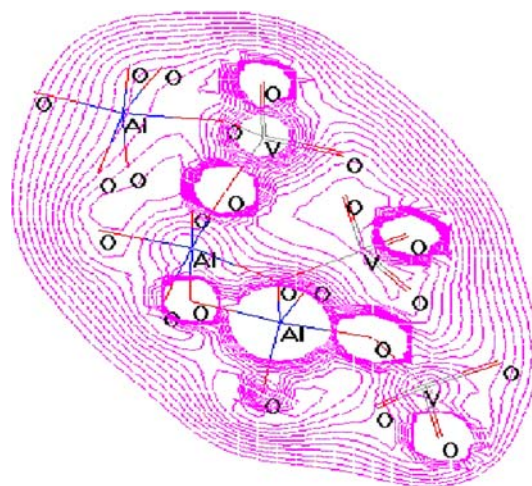


**Fig. 7** Molecular Electrostatic Potential (MEP) distribution for  $[\text{Al}_3\text{V}_3\text{O}_{23}]^{18-}$

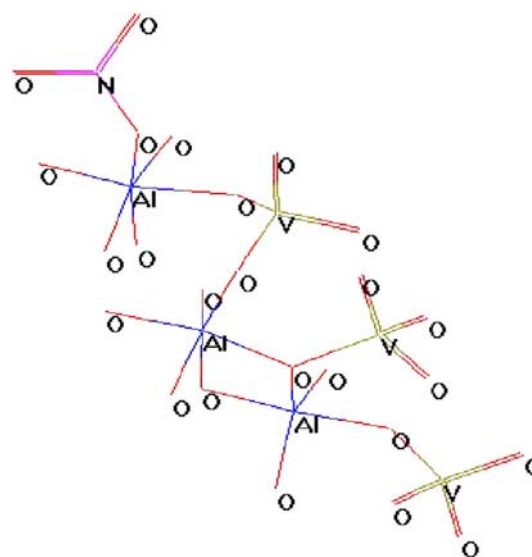


**Fig. 8** The possible interaction between  $\text{AlVO}_4$  and  $\text{NO}_2^-$  groups

theoretical normal modes of vibration. Figure 9 shows the experimental and calculated infra red spectrum, as well as the deconvolution curves. Vertical lines indicate the position of the simulated frequencies and their relative intensity. Gaussian functions were assumed to fit the experimental spectrum using the theoretical positive frequencies. The deconvolution was performed by fixing the position of the calculated frequencies and varying the width and height of the function. This model only reproduces the trend of the experimental spectrum, particularly between  $650$  and  $1,200\text{ cm}^{-1}$ , because a thorough simulation is not possible due to the complex crystal structure of the  $\text{AlVO}_4$ .

**Table 3** Frequencies of theoretical normal modes of vibration

|              |              |        |        |        |        |         |              |              |       |       |       |              |       |       |       |              |
|--------------|--------------|--------|--------|--------|--------|---------|--------------|--------------|-------|-------|-------|--------------|-------|-------|-------|--------------|
| 1139.2       | 1123.2       | 1117.4 | 1103.8 | 1092.1 | 1068.8 | 1053.41 | 1018.4       | 971.0        | 966.9 | 950.3 | 948.1 | 918.9        | 888.5 | 748.8 | 540.1 | 505.63       |
| Al(p)/<br>V2 | Al(h)/<br>V3 | Al(h)  | V3     | V2     | V2     | –       | Al(h)/<br>V1 | Al(h)/<br>V1 | Al(h) | –     | –     | Al(h)/<br>V1 | Al(h) | V3    | V2    | Al(h)/<br>V1 |

Al(h) and Al(p) indicate hexagonal and pentagonal coordinated Al, respectively. Units of wave numbers are given in  $\text{cm}^{-1}$

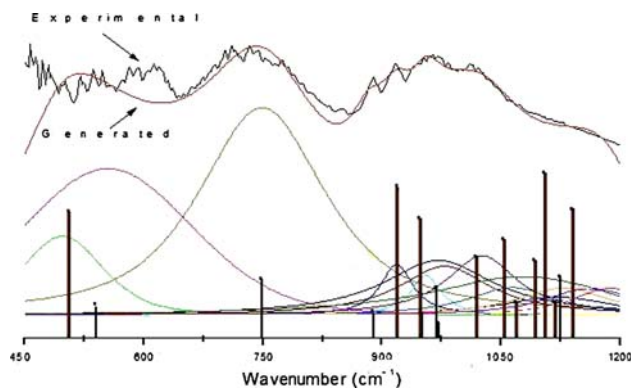


**Fig. 9** Experimental and calculated IR spectrum of  $\text{AlVO}_4$  between 450 and  $1,200 \text{ cm}^{-1}$ . Vertical lines indicate the position of the frequency of normal modes of vibration of the calculated IR. The simulated deconvolution functions are also shown

## Conclusions

The compound  $\text{AlVO}_4$  has been prepared using the sol–gel route, both for powders and thin films. The thin films were deposited on alumina substrates and their electrical characterization was performed. Very similar temperature coefficients of resistivity were obtained for the films prepared with different solutions of the sol in toluene.

The Rietveld refinement of the crystal structure gave excellent agreement between refined and calculated X-ray spectra, assuming that  $\text{AlVO}_4$  is isostructural  $\text{FeVO}_4$ . The derived atomic positions of Al, O and V were used for the quantum-chemical analysis to draw the contour maps of the HOMO and LUMO of the chain  $[\text{Al}_3\text{V}_3\text{O}_{23}]^{18-}$ . According the model described, the  $\text{NO}_2$  groups form the second coordination sphere of six-coordinated atoms of Al, during the absorptive processes.

The vibrational spectrum was also calculated and compared with the experimental one. It is possible to reproduce the experimental IR of  $\text{AlVO}_4$  in the range from  $650$  to  $1,200 \text{ cm}^{-1}$ , but a complete simulation is not possible because of the complex structure of  $\text{AlVO}_4$ .

**Acknowledgments** The authors thank the Laboratorio de Materiales of the Facultad de Ciencias, UASLP (San Luis Potosí, Mexico) for the IR measurements and Prof. G. Sberveglieri and Dr. C. Baratto (Dipartimento di Chimica e Fisica per l'Ingegneria dei Materiali, Università di Brescia) for the useful discussion.

## References

1. Isihara T, Shiokawa K, Eguchi K, Arai H (1989) *Sens Actuators* 19:259
2. Rao N, van den Bleek CM, Shoonman J (1993) *Solid State Ionics* 59:263
3. Brásdová V, Verónica Ganduglia-Pirovano M, Sauer J (2005) *J Phys Chem B* 109:394
4. Leyer B, Schmeltz H, Göbel H, Meixner H, Scherg T, Knözinger H (1997) *Thin Solid Films* 310:228
5. Pohle R (2000) Dissertation. Technische Universität, München
6. Arisi E (2000/2001) Thesis. Facoltà di Scienze Matematiche, Fisiche e Naturali, Università degli Studi di Parma, Italy
7. Ekambara S, Patil KC (1995) *J Alloys Comps* 217:104
8. Yamaguchi O, Uegaki T, Miyata Y, Shimizu K (1987) *J Am Ceram Soc* 70:C198
9. Baran EJ, Botto IL (1977) *Monatsh Chem* 108:311
10. Ferrari M, Lutterotti L (1994) *J Appl Phys* 76:7246
11. Arisi E, Palomares Sánchez SA, Leccabue F, Watts BE, Bocelli G, Calderón F, Calestani G, Righi L (2004) *J Mater Sci* 39:2107
12. Fleming I (1976) *Frontier orbitals and organic chemical reactions*. John Wiley and Sons, London
13. Anderson WP, Cundari TR, Zerner MC (1991) *Int J Quantum Chem* 39:31